

Research on Damage of Underwater Shock Waves at Multiple Explosion Points to Ships

Conghui Duan

North University of China

Jianping Yin (✉ yjp123@nuc.edu.cn)

North University of China

Zhijun Wang

North University of China

Zhiwei Hao

North University of China

Article

Keywords: Shallow water explosion, More explosive point, Numerical simulation, The ship damage

Posted Date: November 29th, 2022

DOI: <https://doi.org/10.21203/rs.3.rs-2300383/v1>

License: © ⓘ This work is licensed under a Creative Commons Attribution 4.0 International License.

[Read Full License](#)

Abstract

In order to study the impact of shallow water explosion shock wave on the ship damage and the overpressure distribution law under different burst points and different explosive quantity and charge, the TNT column bare charge is selected, based on LS-DYNA finite element software, the underwater explosion model is created, and the numerical simulation study of underwater explosion under different burst points is carried out, and the correctness of the finite element model is verified by comparing with the empirical formula. The results show that: the numerical simulation of the underwater explosion shock wave results affected by the mesh size, the use of explosive diameter of $1/10 \sim 1/5$ of the mesh size can be more accurate simulation results; the use of torpedo scattering mode of operation, the bottom of the middle part of the ship after hitting the damage effect is much greater than when not hit, hit the ship and the head and stern side of one of the best damage effect; only hit the stern sides of the case when, 100kg of explosives can do the same or better than 200kg of explosives damage effect, can save part of the resources. It can provide some reference for the study of shallow water explosion damage to ships and torpedo dispersal operations.

1 Introduction

Military integrated operation has become the main mode of operation in modern times, in which ships play a very important role, and also become the main target of attack. The research of underwater explosion shock wave and bubble damage to ships has always been a hot topic for relevant scholars at home and abroad. The representative early research results in the field of Underwater Explosion are Cole's book Underwater Explosion, which systematically summarizes the research results of underwater explosion before the mid-20th century [1]. Gilmore[2] the partial differential equations for the flow of a compressible liquid is surrounding a spherical bubble are reduced to a single total differential equation for the bubble-wall velocity. Keller[3] forecasts express the bubble radius and period generated by underwater explosions. Benjamin et al. [4] used high-speed photography technology to capture bubble jet phenomenon near the rigid interface for the first time. Zamyshlyayev et al. [5–6] further studied the dynamic load law of underwater explosion based on Cole's research results and established the theoretical prediction model of underwater explosion bubble movement and load. Wenbin Gu et al. [7–10] summarized the influence of interface and bottom on the explosion shock wave in shallow water through experimental research. Rajendran et al. [17–18] conducted a series of underwater explosion tests near steel plates to study the response and failure phenomenon of steel plates under different blast distances. Zhang A M et al. [19–22] mainly conducted a series of studies on the three-dimensional state of underwater explosion bubbles, formed a relatively complete theory of underwater explosion bubble pulsation, analyzed the load characteristics of underwater explosion, and summarized the damage characteristics of underwater explosion on ship structure. In general, the research on the front underwater explosion is mainly focused on the study of different depth and different charge equivalents. There are few studies on the damage effect of underwater explosion at multiple detonation points and different explosion positions, so further research is needed in this aspect.

This paper will study the damage law of the shock wave caused by the shallow water explosion with multiple detonation points to the ship, and get the distribution range of the blast wave and the attenuation law of the shock wave at different detonation points, as well as the damage effect of the ship, so as to provide a certain reference for the analysis and research of the damage caused by underwater explosion to the ship and the torpedo spread battle.

2 Numerical Calculation Model

2.1 Finite element model

The finite element software LS-DYNA was used to simulate the shallow water explosion. TNT spherical charge was used for the explosive, and the density was 1.63g/cm³. All the explosion points were located at a depth of 10 m from the water. Suppose that the underwater depth is 28 m, the height of the air domain is 20 times of the charging radius, and the ship's cabin model adopts the strength equivalence method equivalent to 1/2 hull, with the equivalent model size of 64 m×15 m×12.8 m. The structure diagram is shown in Fig. 1, and the finite element model diagram is shown in Fig. 2. The simulation uses the keywords INITIAL_VOLUME_FRACTION_GEOMETRY and INITIAL_DETONATION to realize spherical charge and central detonation, respectively.

The Euler algorithm is used to set the Flow-Out boundary to realize the outflow of the Euler field boundary material. Select the material model directly from the material library, using the ideal air state equation:

$$P = (\gamma - 1)\rho e$$

In the formula: P is the air pressure, take the standard atmospheric pressure; γ is the ideal gas thermal insulation index, take 1.4; ρ is the air density, take $1.225 \times 10^{-3} \text{g/cm}^3$; e is the initial specific internal energy of the air, take $2.068 \times 10^5 \text{J/m}^3$. TNT explosive uses JWL equation of state and JWL equation of state is:

$$P = A \left(1 - \frac{\omega}{R_1 V} \right) e^{-R_1 V} + B \left(1 - \frac{\omega}{R_2 V} \right) e^{-R_2 V} + \frac{\omega E_0}{V}$$

In formula P is the pressure generated by explosive explosion; V is the relative volume; E_0 is the internal energy per unit volume; A, B, R_1, R_2, ω are the material parameters. Air is described by the linear polynomial equation of state, $C_0 \sim C$ is the linear polynomial equation of state parameter, and E_0 is the initial unit mass internal energy of air; water is described by the Gruneisen equation of state, and the pressure of the compressed material is defined as:

The pressure defining the expansion material is defined as:

C, S_1, S_2, S_3 are the Gruneisen equation of state parameters; γ_0 is the Gruneisen constant; $\mu = \rho/\rho_0 - 1$; α is the first-order volume correction of γ_0 . The soil is described by a linear elastic model, E is the elastic

modulus and G is the shear modulus; the blank material is defined by the keyword MAT_ALE_VACUUM. The material parameters are shown in Table 1.

Table 1
Material Parameters

Material	$D/(m/s)$	A/GPa	B/GPa	R_1	R_2	ω	$E_0/(J/m^3)$
TNT	6930	373.77	3.7471	4.15	0.9	0.35	6.62×10^{10}
Material	$\rho/(kg/m^3)$	$C_0 \sim C_3$	C_4	C_5	C_6	$E/(J/kg)$	
Air	1.225	0	0.4	0.4	0	2.5×10^5	
Material	$P_0/(kg/m^3)$	C	S_1	S_2	S_3	γ_0	E
Water	1 000	1 480	2.56	-1.986	0.2268	0.5	$2.895e^{-6}$

This study mainly designed five working conditions according to the location and number of different blast points. W is the explosive equivalent, H is the explosion depth, n is the cumulative number of explosion loading, the bottom center is the (0,0) point, the upward to the right is the positive coordinate, and G is the explosion point coordinate. The specific working conditions are shown in Table 2:

Table 2
Calculation parameters for each working condition

No.	W/kg	H/m	n	G
1	200	100	1	(0, -100)
2	200	100	2	(-50, -100) 50, -100
3	100	100	2	(-50, 100) 50, -100
4	200	100	2	(0, -100) 50, -100
5	200	100	3	(-50, -100) 0, -100 50, -100

2.2 Mesh Sensitivity

The efficiency and accuracy of numerical simulation are closely related to the size of the grid. In order to obtain the appropriate grid size, we designed four sets of numerical simulations of underwater explosion with different grid sizes. Considering the large simulation model and computation time, the grid sizes selected are 10, 15, 20 and 40 cm, respectively. Based on a large number of tests, the empirical formula of peak underwater shock wave pressure is as follows:

$$P_m = k \left(\frac{\sqrt[3]{\omega}}{r} \right)^\alpha$$

Formula: P_m is the shock wave peak pressure (MPa); ω is the explosive mass (kg); r is the explosive distance from the starting point to the ship target; k is the explosive related empirical coefficient; α is the explosive related empirical coefficient. For different explosives, the associated Cole explosion parameters k and α are shown in Table 3.

Table 3
Cole explosion parameters of different charges

Explosive	TNT	THL	HBX-1	PENT	NSTHL
k	53.3	63.48	53.51	56.21	67.08
α	1.13	1.144	1.18	1.194	1.26

Figure 3 shows the simulation results of the peak pressure and the empirical formula of the shock wave generated from the underwater 100kgTNT explosion at different grid sizes. As can be seen from the figure, with the increase of grid size near field shock wave peak pressure drop obviously, the curve is steep slope, the far field shock wave downward trend stabilized, 20 cm simulation results and empirical formula curve is consistent, the deviation is small, so the simulation grid choose 20 cm grid size, the simulation results error within a reasonable range, the result is more accurate and feasible.

2.3 Establish A Numerical Calculation Model

Table 4 shows the simulation results and the empirical formula theoretical results of the 100 kg TNT explosive explosion at 10 m underwater. The P_m is the peak pressure of the shock wave. The simulation results and the theoretical results agree with an average error of 3.13, so the simulation results have high reliability.

Table 4
Comparison of the numerical and theoretical results

P_m			
S/m	Theoretical Results/MPa	Numerical Results/MPa	Error/%
2	135.05	137.36	1.72
4	61.71	62.39	1.10
6	39.03	38.78	0.64
8	28.20	27.21	3.51
10	21.91	20.80	5.07
12	17.83	17.21	3.48
14	14.98	14.02	6.40

3 Numerical Simulation Results

3.1 Analysis of shock wave overpressure peak rule

The cloud map of the bottom pressure of the five final conditions was calculated by simulation, as shown in Fig. 4.

According to the pressure cloud diagram, we can find that the pressure at the bottom of the ship at the final moment of different working conditions is funnel shaped, and all of them are symmetric about the horizontal plane direction except for the fourth working condition. Working condition of the maximum shock wave pressure on a location for the bottom near the center position, and gradually spread to ship week, working condition of shock wave pressure maximum location for the center of the bottom and the bottom four angular position, and then the several points centered around to abate, working condition of shock wave pressure on three biggest position as close to the center of the bottom and the bottom four angular position, The rest are weakened at the center of these points. The maximum position of shock wave pressure in working condition 4 is around the bottom of the ship on the side of the explosion point, and the maximum position of shock wave pressure in working condition 4 is around the bottom of the ship and the four corners. The order of maximum shock wave pressure from high to low is condition 5 > condition 4 > condition 1 > condition 2 > condition 3.

3.2 Hull elevation analysis

In order to explore the extent of the hull was elevated after the underwater explosion and to judge the damage efficiency, the maximum elevation waterfall map of different conditions was obtained from the simulation results, as shown in Fig. 5.

It can be concluded from the perspective of Fig. 5 that the elevation degree of the hull is ranked from high to low to condition 1 > condition 4 > condition 2 > condition 3 > condition 5. The shock wave has the most obvious effect on the hull lifting, the condition 5 has the worst effect, and the other effects are similar.

3.3 Analysis of the maximum deformation position of the ship bottom

The curve diagram of the maximum deformation position of the ship bottom is calculated by simulation, as shown in Fig. 6.

As can be seen from Fig. 6, the maximum deformation degree is sorted from high to low to condition 3 > condition 5 > condition 1 > condition 4 > condition 2. It can be seen from Fig. 7 that the shape change of the pressure curve of condition 2 and condition 4 is similar, and the shape changes of the maximum deformation position of condition 1 and condition 3 are similar.

The maximum pressure, deformation degree and elevation degree of the hull on the bottom of each working ship can directly compare the advantages and disadvantages of each working condition, as shown in Fig. 8.

As can be seen from Fig. 8, the index of condition 1 and condition 4 is more balanced and higher in all aspects, and the damage effect on the whole hull is better.

4 Conclusion

In this paper, through numerical simulation of different detonation locations and quantities, the damage analysis of ships caused by underwater explosion at different detonation points is studied. Through comparison and verification with empirical formulas, a conclusion is drawn:

- (1) The numerical simulation results of underwater explosion shock wave are affected by the grid size, and the simulation results can be obtained more accurately by using the grid size of $1/10 \sim 1/5$ of the explosive diameter.
- (2) The damage effect after hitting the middle part of the bottom of the ship is much greater than that without hitting, and the damage effect of hitting the middle part of the ship and one side of the head and tail is the best.
- (3) In the case of only hitting both sides of the stern, the damage effect of 100kg explosive can be as good as or even better than that of 200kg explosive, which can save some resources.

Declarations

Data Availability

The data that support the findings of this study are available from the corresponding author upon reasonable request.

Conflicts of Interest

The authors declare that they have no conflicts of interest.

Funding Statement

The authors would like to acknowledge the financial support for the project supported by Shanxi Province Graduate Education Innovation project in 2021 no. 2021Y575.

References

1. COLE R H. Underwater explosion [M]. New Jersey: Princeton University Press, 1948: 118–127.
2. Gilmore F R. The growth or collapse of a spherical bubble in a viscous compressible liquid [J]. California Institute of Technology, 1952.
3. Keller J B, Kolodner I I. Damping of Underwater Explosion Bubble Oscillations [J]. Journal of Applied Physics, 1956, 27(10): 1152–1161.
4. BENJAMIN T B, ELLIS A T. The collapse of cavitation bubbles and the pressures thereby produced against solid boundaries [J]. Philosophical Transactions of the Royal Society of London, 1966, 260(1110): 221–240.
5. ZAMYSHLYAYEV B V, YAKOVLEV Y S. Dynamic loads accompanying an underwater explosion [M]. Sudostroyeniye, Leningrad, 1967.
6. ZAMYSHLYAYEV B V. Dynamic loads in underwater explosion: AD-757183 [R]. 1972: 86–120.
7. GU W B, YE X S, ZHANG P X, et al. Experimental studies of bottom influence in shallow layer water explosion [J]. Journal of PLA University of Science and Technology, 2001, 2(2): 55–58.
8. GU W B, YE X S, LIU W H, et al. Peak pressure investigation of exploding wave influenced by interfaces in shallow-layer water [J]. Journal of PLA University of Science and Technology, 2001, 2(5): 61–63.
9. GU W B, ZHENG X P, LIU J Q, LI D J, LU M. Experimental study on oblique impact of explosion shock wave on concrete pier in shallow water [J]. Explosion and shock, 2006(04): 361–366.
10. GU W B, MA H Y, TANG Y, et al. Influence of water bottom on the explosion effect of shallow-layer water charging [J]. Blasting, 2003, 20(4): 88–92.
11. ZHANG Z H, ZHU X, BAI X F. The study on numerical simulation of underwater blast wave [J]. Explosion and Shock Waves, 2004, 24(2): 182–188.
12. FANG B, ZHU X, ZHANG Z H, et al. Effect of parameters in numerical simulation of underwater shock wave [J]. Journal of Harbin Engineering University, 2005, 26(4): 419–424.

13. ZHU X, MU J L, HONG J B, HUANG X M, LI H T. Experimental study on bubble pulsation characteristics of underwater explosion. *Journal of Harbin Engineering University*, 2007(04): 365–368.
14. FANG B, ZHU X. Numerical simulation of underwater explosion bubble with different boundaries [J]. *Journal of Naval University of Engineering*, 2008, 20(2): 85–90.
15. ZHU X, MU J L, WANG H, ZHANG Z H. Damage mode of stiffened plate under underwater explosion load [J]. *Explosion and shock*, 2010, 30(03): 225–231.
16. YUAN J H, ZHU X, ZHANG Z H, et al. Numerical simulation method study of underwater explosion load [J]. *Ship Science and Technology*, 2011, 33(9): 18–23.
17. RAJENDRAN R, NARASIMHAN K. Deformation and fracture behaviour of plate specimens subjected to underwater explosion—a review [J]. *International Journal of Impact Engineering*, 2006, 32(12): 1945–1963.
18. RAJENDRAN R, LEE J M. Blast loaded plates [J]. *Marine Structures*, 2009, 22(2): 99–127.
19. ZHANG A M. 3D Dynamic behavior of underwater explosion bubble [D]. Harbin: Harbin Engineering University, 2006: 2–5.
20. ZHANG A M, YAO X L. The effect of charge and water depth on the underwater explosion bubble [J]. *Engineering Mechanics*, 2008, 25(3): 222–229.
21. LI S, ZHANG A M, HAN R. Numerical analysis on the velocity and pressure fields induced by multi-oscillations of an underwater explosion bubble [J]. *Chinese Journal of Theoretical and Applied Mechanics*, 2014, 46(4): 533–543.
22. ZHANG A M, WANG S P, WANG Y, YAO X L. Survey on the characteristics of underwater explosion damage to ship structure [J]. *China Ship Research Institute*, 2011, 6(03): 1–7.

Figures

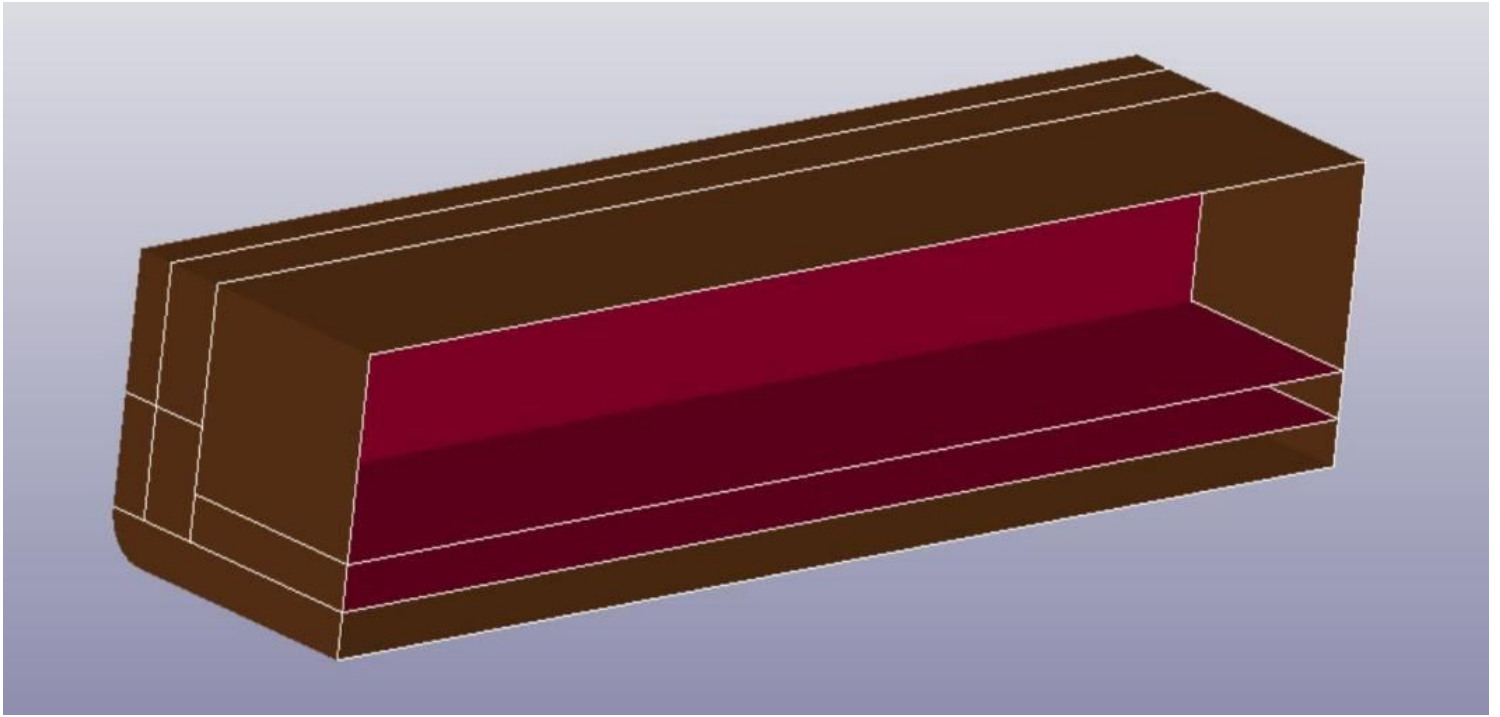


Figure 1

The cabin finite element model

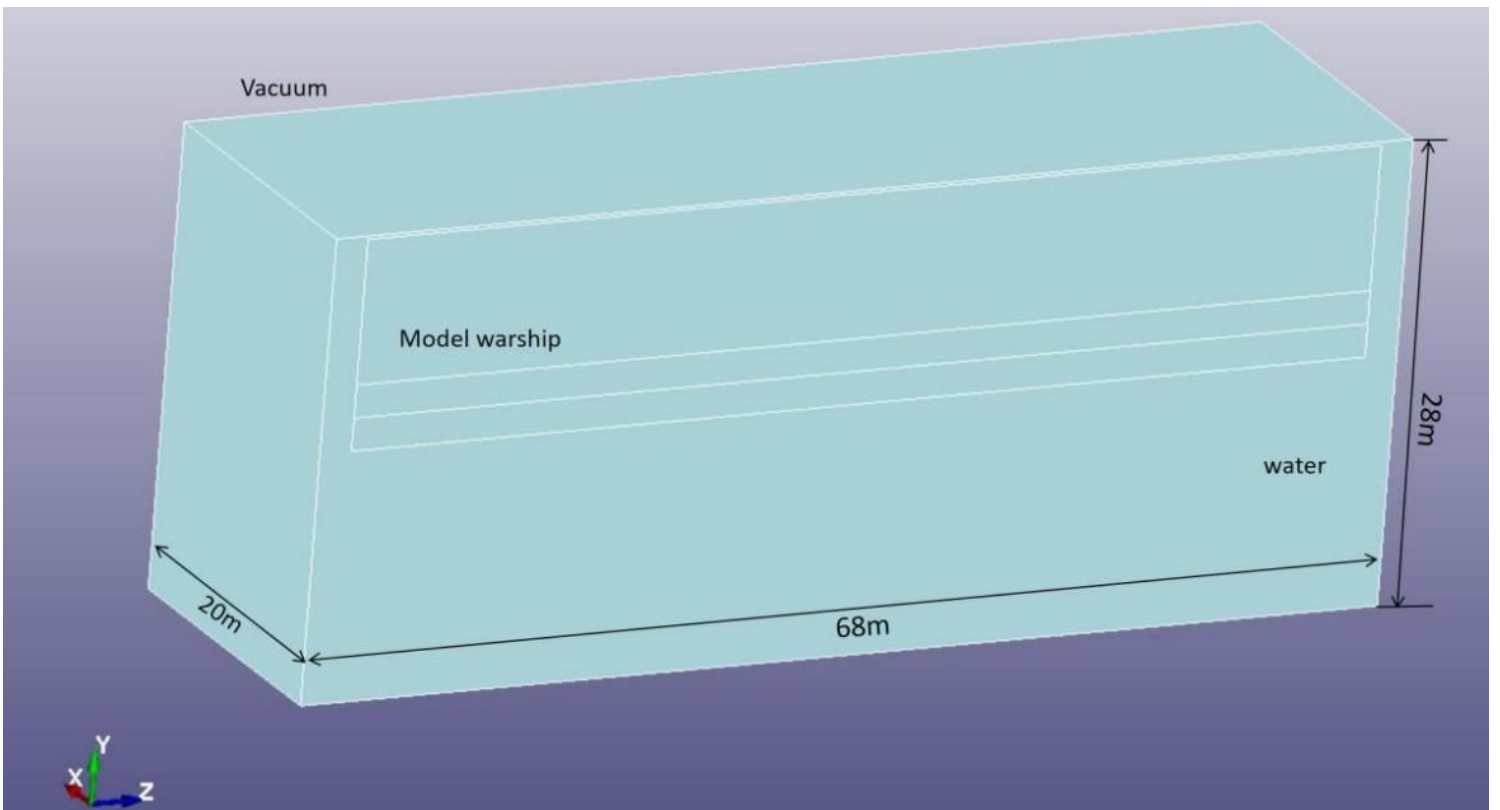


Figure 2

Schematic representation of the FEM calculation model

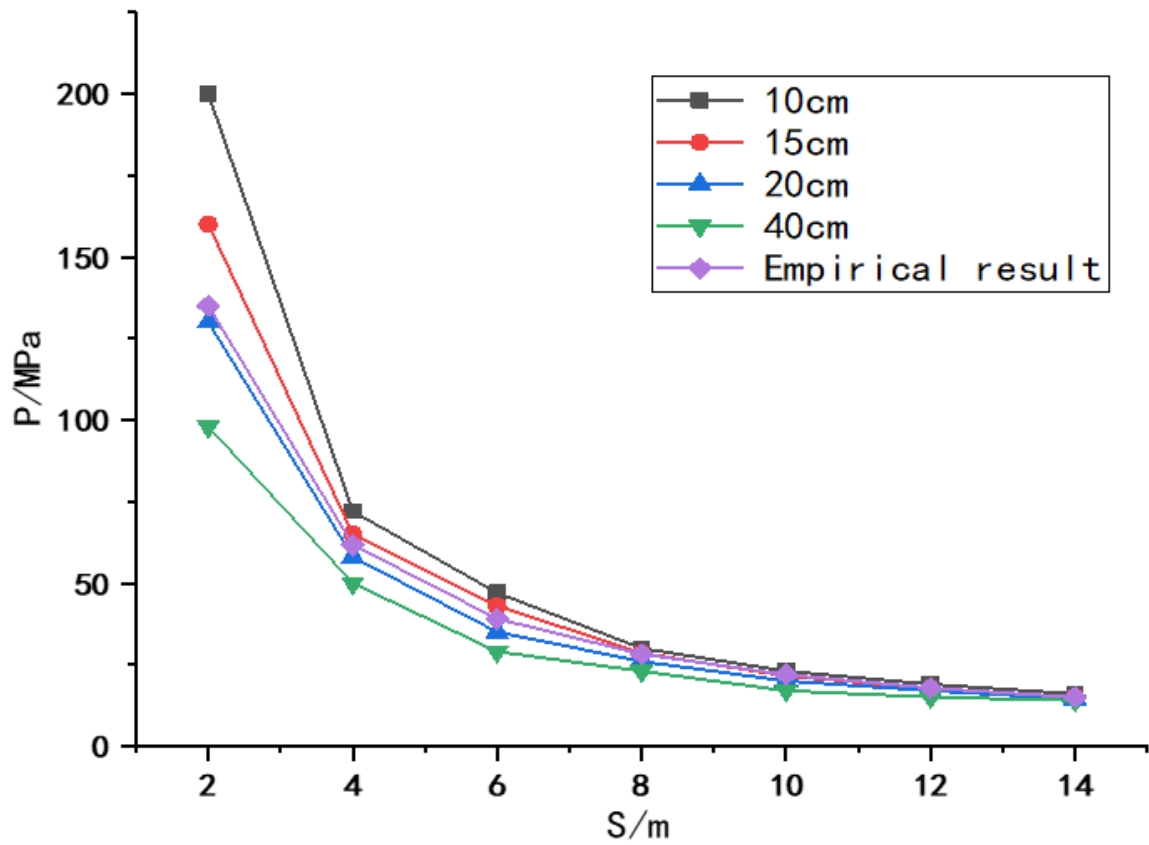


Figure 3

Shock wave peak pressure at different grid sizes

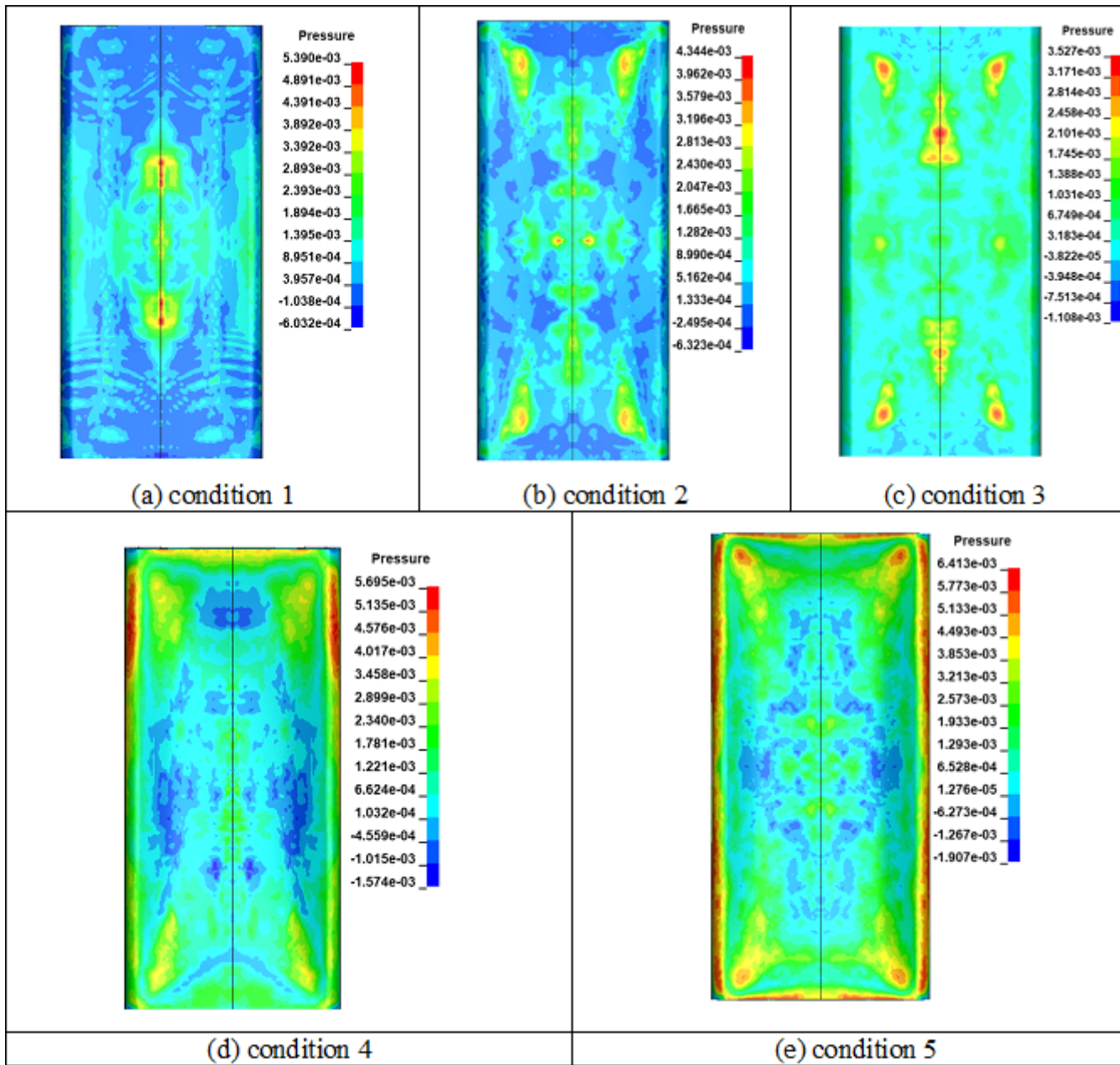


Figure 4

Final bottom bottom bottom bottom bottom moment

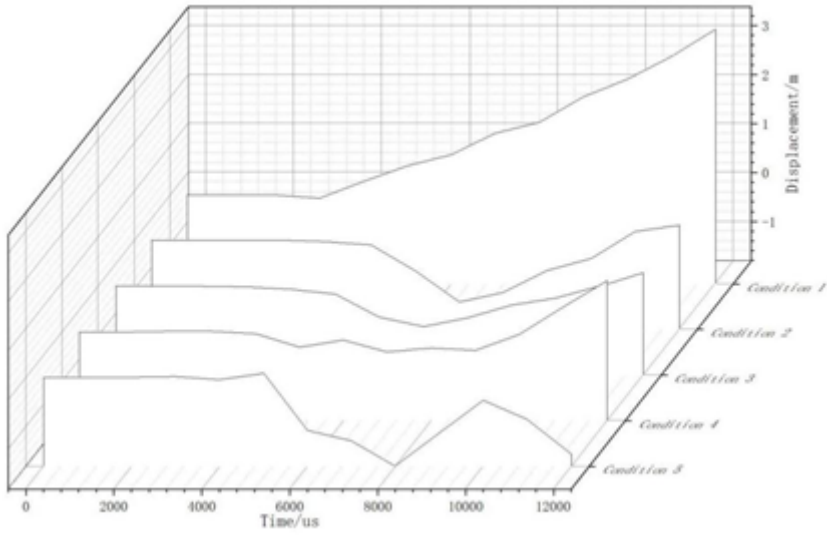


Figure 5

Maximum elevation waterfall diagram for each working condition

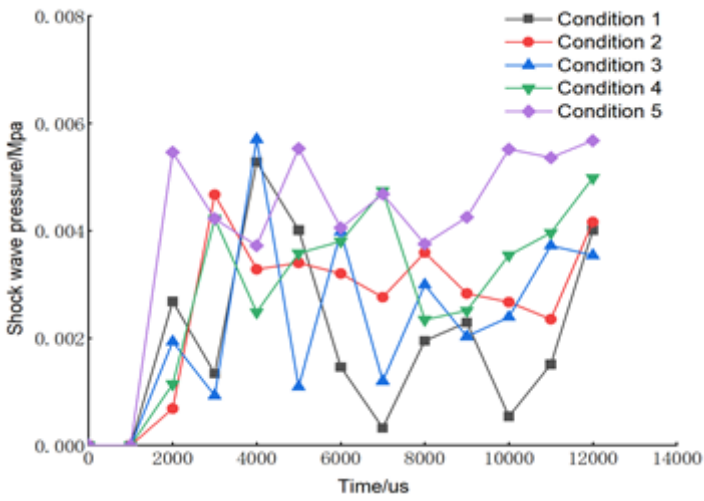


Figure 6

Pressure curve of the maximum deformation position of the ship bottom

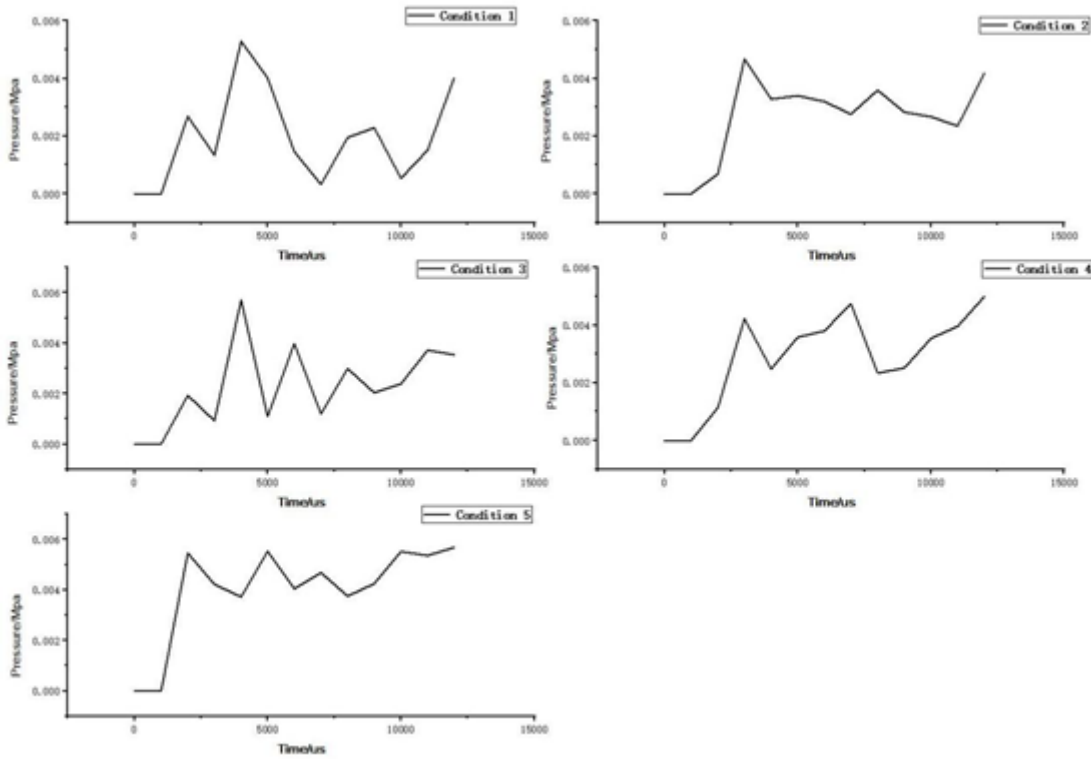


Figure 7

Pressure line diagram of maximum deformation position of boat bottom under each condition

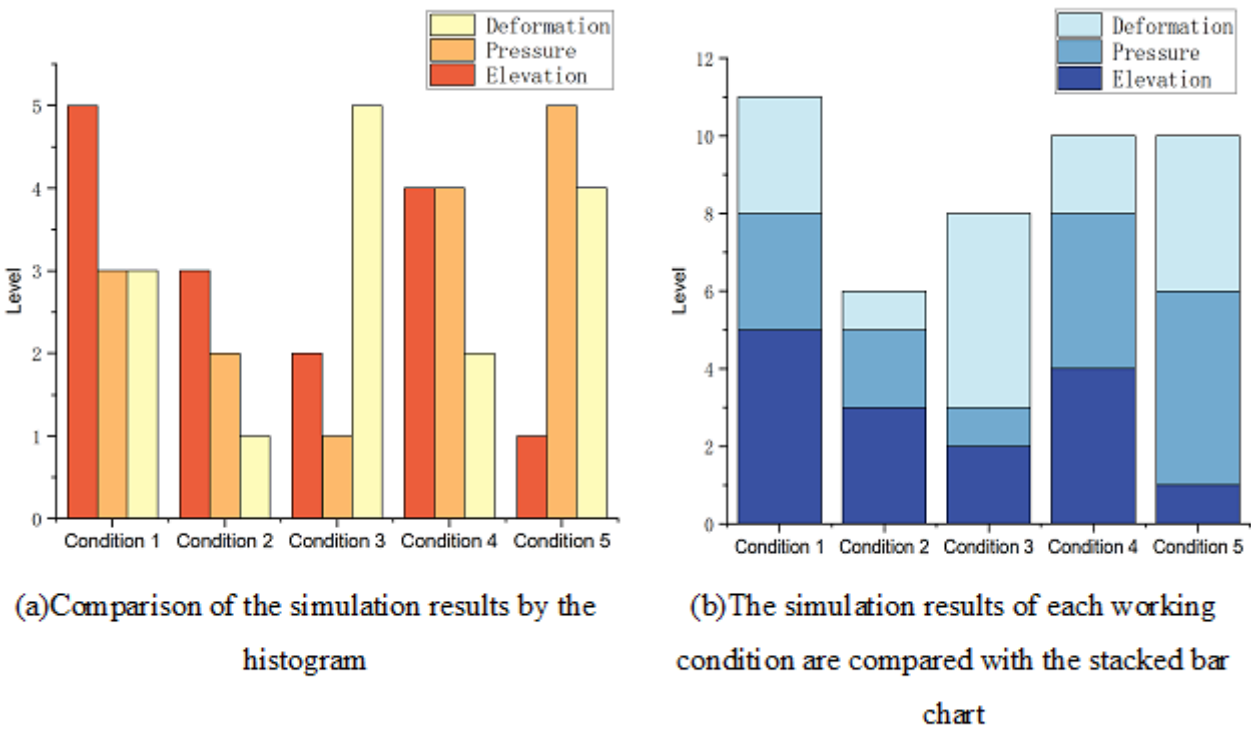


Figure 8

Comparison diagram of each working condition